

Elucidating the Reduction Mechanism of Lithium Bis(oxalato)borate

Tim Melin,* Robin Lundström, and Erik J. Berg*




Cite This: *J. Phys. Chem. Lett.* 2024, 15, 2537–2541



Read Online

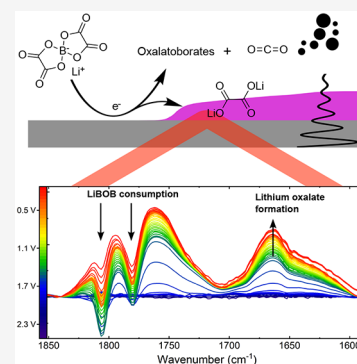
ACCESS |

 Metrics & More

 Article Recommendations

 Supporting Information

ABSTRACT: Electrolyte additives are indispensable to enhance the performance of Li-ion batteries. Lithium bis(oxalato)borate (LiBOB) has been explored for many years, as it improves both cathode and anode performance. No consensus regarding its reaction mechanisms has, however, been established. A model *operando* study combining attenuated total reflection infrared spectroscopy (ATR-FTIR), electrochemical quartz crystal microbalance (EQCM), and online electrochemical mass spectrometry (OEMS) is herein presented to elucidate LiBOB reduction and electrode/electrolyte interphases thus formed. Reduction of the BOB^- ion sets in at ~ 1.8 V with solid lithium oxalate and soluble oxalatoborates as the main products. The reduced BOB^- ion also reacts with itself and its environment to evolve CO_2 , which in turn impacts the interphase formed on the negative electrode. This study provides further insights into the reduction pathways of LiBOB and how they contribute to the interphase formation.



Optimizing electrolyte composition is paramount for advancing Li-ion batteries. Additives are commonly introduced to fulfill the various functions necessary for Li-ion cell chemistry. Three main categories of additives are electrode/electrolyte interphase formers (on both anode and cathode), harmful species scavengers, and stabilizer agents.¹ Additives are typically soluble in the electrolyte and come in the form of either a molecule or a salt. Lithium bis(oxalato)borate (LiBOB, Figure S1 and to the left in Figure 4) has garnered tremendous attention for its promising layer-forming properties on not only the anode but also the cathode.^{2,3} LiBOB was synthesized and patented in 1999 by Lischka et al.⁴ and has been studied extensively by Xu et al.^{5–11} among many others. One aspect of LiBOB that differs from many other additives is its relatively high reduction potential. Most layer-formers are being reduced at the anode at potentials close to the reduction potential of the electrolyte solvent ethylene carbonate (EC) < 0.9 V.¹ LiBOB on the other hand, is reported to be reduced from 1.8–1.0 V,^{10,12–14} well before EC and many other additives, such as the well-known vinylene carbonate and fluoroethylene carbonate.¹ Several reaction pathways have been proposed for the reduction of LiBOB, but most are similar and suggest the formation of lithium oxalate ($\text{Li}_2\text{C}_2\text{O}_4$) and carbon dioxide (CO_2) as the main reaction products. Apart from pure $\text{Li}_2\text{C}_2\text{O}_4$, more complex molecular combinations of oxalate borates and boron-containing semicarbonates have been proposed. Reduced BOB^- species have also been suggested to react with carbonate solvents (e.g., EC) to form boron-containing semicarbonates¹³ and oligomers/polymers.¹⁴ The synthesis of LiBOB has shown to be somewhat challenging, and boron-containing impurities from synthesis have also been claimed to be the cause for the reduction at high potentials (>1.7 V).^{15,16}

The primary focus of the study presented herein is to elucidate the reduction pathway of the BOB^- anion and comprehend the properties of the solid electrolyte interphase (SEI) thus formed in the process. Important is the effectiveness of the LiBOB-derived SEI in suppressing electrolyte degradation and accommodating the negative influence of typical contaminants like water. Most studies conducted to date on LiBOB performed *ex situ* or *post-mortem* chemical analysis of the SEI after Li-ion cell formation and/or after prolonged cycling by subjecting the electrode extracted from the cell to various spectroscopic (e.g., X-ray photoelectron spectroscopy, vibrational spectroscopy)^{7,9,10,12,14,17,18} or microscopic (e.g., transmission electron microscopy)¹³ techniques. SEI formation is, however, well-recognized to be a complex multistep process, hardly captured by *ex situ* analytical approaches. Therefore, a set of complementary *operando* characterization techniques, namely, attenuated total reflection infrared spectroscopy (ATR-FTIR), electrochemical quartz crystal microbalance (EQCM), and online electrochemical mass spectrometry (OEMS), are here applied to monitor solid, liquid, and volatile reaction products, respectively, associated with LiBOB reduction during operation of the cell.

Figure 1 shows the results from *operando* ATR-FTIR of a 50 mM LiBOB containing a model electrolyte. Compared with a classic Li-ion electrolyte, the cathodically more stable LiClO_4

Received: February 1, 2024

Revised: February 20, 2024

Accepted: February 22, 2024

Published: February 28, 2024



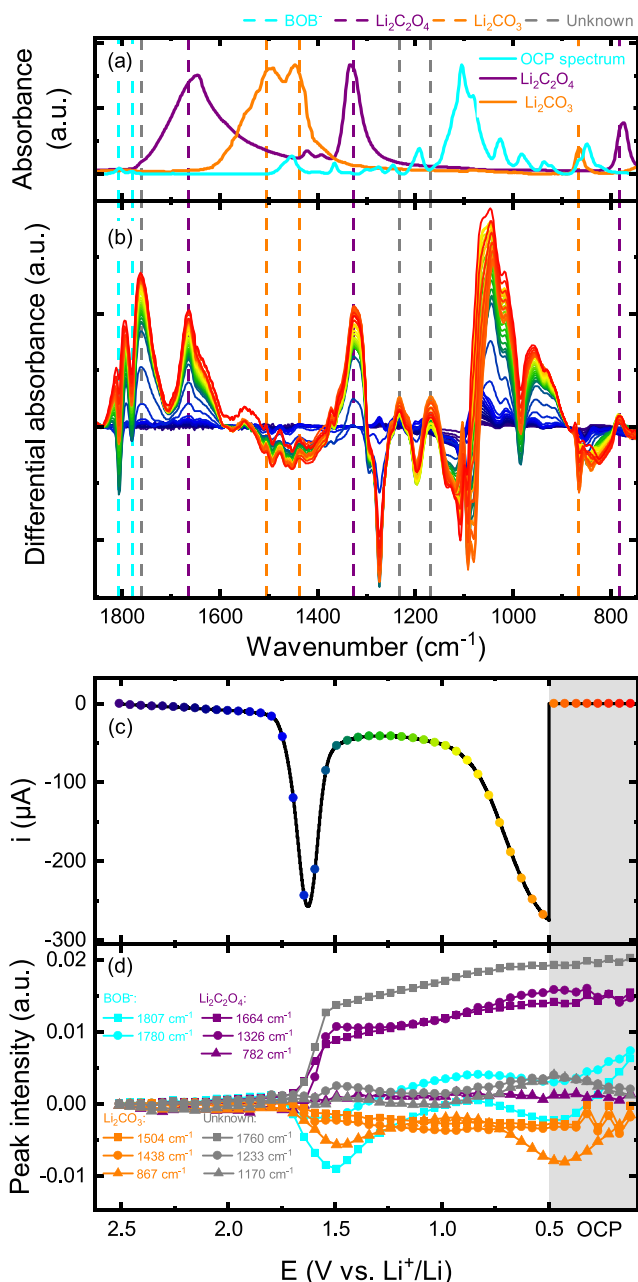


Figure 1. (a) Reference absorbance spectra of a porous GC soaked in 0.2 M LiClO₄ in DME + 50 mM LiBOB at OCP (“OCP spectrum” in figure), Li₂C₂O₄, and Li₂CO₃, (b) *operando* IR differential absorbance spectra relative to a spectrum at open-circuit potential (OCP) with corresponding (c) linear sweep voltammogram of a porous GC electrode pressed on a diamond ATR crystal in 0.2 M LiClO₄ in DME + 50 mM LiBOB and (d) peak intensities of selected wavenumbers as a function of electrode potential. Spectral color coding in panel b corresponds to data points in panel d.

salt dissolved in DME was applied to avoid the complexity of organic carbonate solvent decomposition and the extensive side-reactions of LiPF₆. In order to ensure the purity of the LiBOB salt used herein, ¹¹B-NMR was performed on pure salt dissolved in DMSO, and only one signal was observed and assigned to LiBOB (Figure S2). A significant influence from impurities remaining after the LiBOB synthesis is therefore unlikely. A porous glassy carbon (GC) composite working electrode was applied as an electrode to mimic the surface of

the typical graphite Li-ion active material, but at the same time avoid effects associated with cosolvent Li⁺ intercalation. As the GC electrode was pressed against an ATR crystal, both the electrode surface and the electrolyte phase were probed. During linear sweep voltammetry (LSV), all spectra recorded were found to be dominated by vibrations from various electrolyte species (OCP spectrum in Figure 1a and Figure S3). Therefore, differential absorbance spectra (relative to a spectrum at the OCP) are presented in Figure 1b to amplify spectral changes. The current recorded during LSV from the OCP to 0.5 V (Figure 1c) shows a clear reduction peak setting in at 1.8 V associated with BOB⁻. Eleven spectral features (vertical dashed lines in Figure 1a,b) are identified, and their respective intensities are tracked as a function of electrode potential (Figure 1d).

The spectra remain more or less unchanged from those of the OCP until the reduction current sets in at 1.8 V, except for minor changes in the ratio between Li⁺-coordinated and free DME, likely as a consequence of Li⁺ adsorption to GC during the negative polarization. Both positive and negative going peak intensities appear <1.8 V and are related to vibrational bands from newly formed or consumed species, respectively. A majority of positive peaks pair with one or multiple negative peaks and are simply attributed to changes in the ratio between free and Li⁺-coordinated DME. For instance, a set of peaks found in the range of 900–1150 cm⁻¹ are dominated by the C–O vibration modes of free and coordinated DME, respectively. Deconvoluting these changes in the electrolyte from emerging bands from new species is limited by the breadth and overlap of these features. Even though this is the case for the majority of positive peaks, a few new peaks with little to no overlap with DME can be analyzed. Two peaks at 1807 and 1780 cm⁻¹ are assigned to valence vibrations of the C=O bond in BOB⁻ (in accordance with the literature¹⁹) and display a rapid drop in intensity <1.8 V, which shows that BOB⁻ is being consumed in the reduction process (Figure 1d). When that reduction process ends <1.5 V the intensity of the same peaks increases due to replenishment of BOB⁻ lost at the electrode surface from the bulk electrolyte, thus implying that only a minor fraction of BOB⁻ at the electrode surface undergoes reduction. A second intensity decrease for BOB⁻ sets in <0.8 V, but now as a result of the consumption of Li⁺ ions due to its stronger adsorption on the GC electrode. After the LSV, the intensity associated with BOB⁻ increases continuously throughout the whole OCP step, reaching even higher intensities than in the OCP spectrum. During BOB⁻ reduction, three strong peaks emerge at 1664, 1326, and 780 cm⁻¹, which agree with the spectrum of Li₂C₂O₄. These peaks grow fast during reduction, but they slow down <1.5 V when no reductive current flows and remain unchanged during the OCP step; that is, no conversion or dissolution of Li₂C₂O₄ is observed. Along with the formation of Li₂C₂O₄, another set of peaks emerges at 1504, 1438, and 867 cm⁻¹, which are assigned to Li₂CO₃. However, these features are very small and overlap with the spectra of the OCP and are therefore not considered to be a major reduction product of BOB⁻. The intensity of 867 cm⁻¹ does not follow the same trend as the other two but resembles the profile of the BOB⁻ vibration, demonstrating the difficulties induced by spectral overlaps. Three additional peaks emerge <1.8 V at 1760, 1233, and 1170 cm⁻¹ and follow the same trend as the Li₂C₂O₄ vibrations, hence suggesting that these three peaks are associated with the remaining oxalatoborates from BOB⁻ reduction, as outlined

below. The interaction between reduced BOB^- and EC was studied with operando FTIR by assembling cells with 0.2 M LiClO_4 in DME + 50 mM LiBOB + 5 vol % EC as electrolyte. Unfortunately, no clear additional features besides the ones already discussed in the sections above could be deconvoluted (Figure S4).

Figure 2 shows the cyclic voltammograms along with the corresponding mass change Δm and calculated mass per

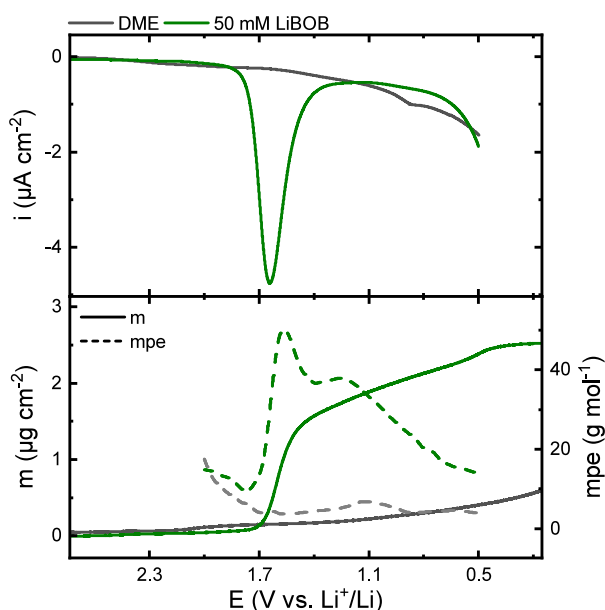


Figure 2. Cyclic voltammograms of carbon-coated QCM sensors in 0.2 M LiClO_4 in DME with and without 50 mM LiBOB with corresponding mass deposition on the sensors and calculated mpe values during the negative sweep.

electron (mpe, grams of deposit per mol electrons) value of carbon-coated QCM sensors cycled in the DME electrolyte including no additive and 50 mM LiBOB. Neither current peaks nor significant mass deposition were recorded when LiBOB was absent, hence confirming the cathodic stability of LiClO_4 in DME. The voltammogram for the LiBOB containing electrolyte is similar to the IR cell (Figure 1c) containing the same electrolytes with a reduction peak attributed to BOB^- reduction starting at 1.8 V. The current <1 V is lower for LiBOB, which is related to the higher cell impedance induced by the LiBOB-derived SEI formed >1 V. Indeed, Δm increases along with the reduction current and slows down as the current decays. At the same time, the highest mpe value of 50 g mol^{-1} is recorded for the LiBOB electrolyte at the peak in the voltammogram, which again suggests the formation of $\text{Li}_2\text{C}_2\text{O}_4$ possessing a mpe-value of 51 g mol^{-1} (assuming a two-electron per $\text{Li}_2\text{C}_2\text{O}_4$ process). An increase in Δm is observed <1 V with essentially no current flow, except for the adsorption/desorption of Li^+ ions. Again, as noted in the ATR-FTIR experiment above, no electrochemical conversion of lithium oxalate is likely, but rather other chemical reactions possibly involve metastable oxalato-borates and the remaining LiBOB salt.

Figure 3 shows cyclic voltammograms (starting from the OCP and vertex potentials 0.5 and 1.7 V) and associated CO_2 , C_2H_4 , and H_2 gas evolution profiles for GC electrodes cycled in the baseline electrolyte, 50 mM LiBOB, 5% EC, as well as 50 mM LiBOB + 5% EC. EC was added in order to monitor

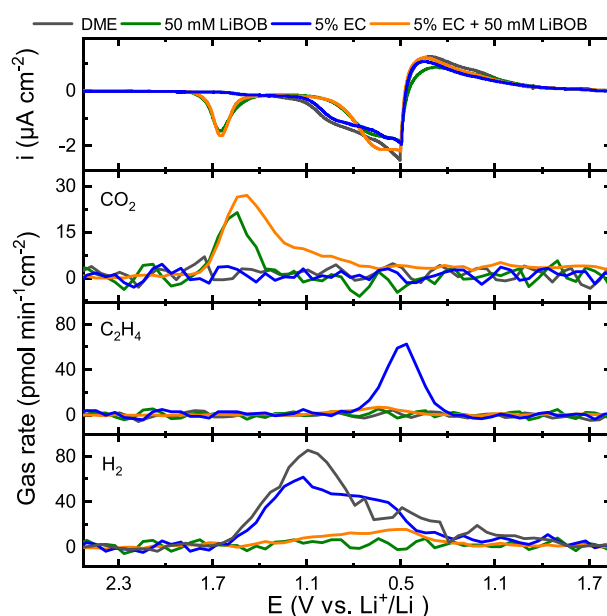


Figure 3. Cyclic voltammograms of GC porous electrodes in 0.2 M LiClO_4 in DME with LiBOB and EC added with corresponding gas evolution rates of CO_2 , C_2H_4 , and H_2 .

LiBOB reactivity toward EC and its ability to suppress EC reduction <0.9 V.¹ Again, a reduction peak starting at 1.8 V is observed when LiBOB is present but now along with the evolution of CO_2 . The total amount of CO_2 evolved is 0.85 nmol cm^{-2} (for 50 mM LiBOB), which is significantly lower than the charge consumed (24.3 $\text{nmol electrons cm}^{-2}$), hence demonstrating that the CO_2 evolution is not a major product of the electrochemical reduction of LiBOB. The addition of LiBOB and generation of CO_2 further suppress H_2 evolution. H_2 is well-known to derive from the reduction of water impurities, but the reduced protons can be scavenged in the presence of CO_2 to form Li-formate rather than inducing hydrogen evolution reaction.²⁰ Compared to LiBOB, the decomposition of EC is much less efficient in generating CO_2 and H_2 evolves similarly to when no additive is present. As expected, EC reduction results in C_2H_4 evolution <1 V. When both LiBOB and EC are present (orange, Figure 3), LiBOB is reduced before EC, which suppresses not only H_2 evolution but also the reduction of EC. Interestingly, more CO_2 evolves when both LiBOB and EC are present, which likely is a result of ring-opening of EC by the reduced BOB^- products. Although the cells display higher impedance, as judged from the magnitude of the reversible currents (Figure 3), the LiBOB-derived SEI on the carbon electrode surface is more passivated and effectively blocks the reduction of both the EC and impurities. This points to the direction that LiBOB provides faster and more effective passivation of the carbon anode compared to EC.

A model study of the electrochemical reduction mechanism of LiBOB, its SEI-forming ability, and chemical side-reactions toward itself and EC is presented and illustrated in Figure 4. A clear reduction peak <1.8 V is observed in all cells containing LiBOB and associated with the formation of an SEI primarily based on Li-oxalate. LiBOB reduction should also result in oxalato-borates along with minor amounts of Li_2CO_3 and CO_2 from subsequent chemical side-reactions between reduced BOB^- species and the rest of the electrolyte. Li_2CO_3 may however likely stem from water impurity reduction and

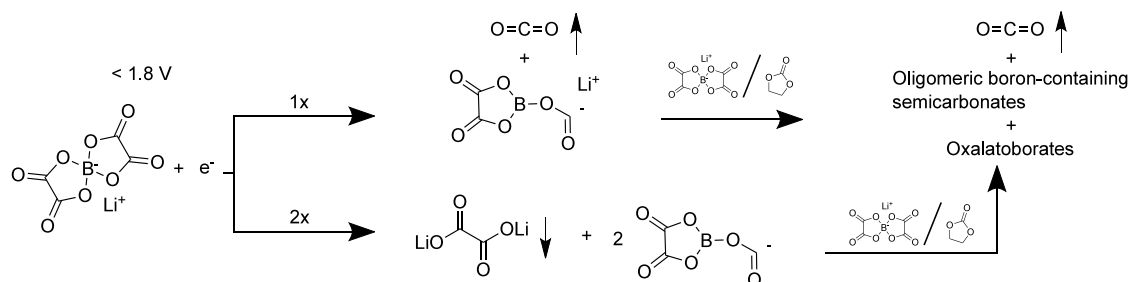


Figure 4. Schematic of two of the possible reduction mechanisms of LiBOB of which products could be identified with OEMS (CO_2 , top) and IR + EQCM ($\text{Li}_2\text{C}_2\text{O}_4$, bottom). The arrows pointing up and down indicate gaseous and precipitating species, respectively.

generation of LiOH, which in turn reacts with the evolving CO_2 . LiBOB is an efficient SEI former, which in spite of a higher cell impedance efficiently suppresses further electrolyte reduction and associated gas evolution. The fundamental insights into reaction pathways of LiBOB and other electrolyte additives are critical to deepen our understanding, advance electrolyte modeling, and accelerate the development of future battery electrolytes. In this study, complementary *operando* techniques are utilized to monitor solid, liquid, and gaseous reaction species during the reduction process of a crucial additive. By doing so, existing uncertainties surrounding the reduction mechanism of LiBOB are addressed. This study not only contributes to fundamental knowledge but also underscores the significance of advancing *operando* techniques. Furthermore, this demonstrates the value of revisiting well-studied systems with novel experimental approaches.

■ ASSOCIATED CONTENT

SI Supporting Information

The Supporting Information is available free of charge at <https://pubs.acs.org/doi/10.1021/acs.jpcllett.4c00328>.

Experimental details and 4 figures: structure of LiBOB (Figure S1), ^{11}B -NMR of LiBOB salt (Figure S2), *operando* IR of 0.2 M LiClO_4 in DME + 50 mM LiBOB (before subtraction of OCP spectrum, Figure S3), and +50 mM LiBOB + 5% EC (Figure S4) (PDF)

Transparent Peer Review report available (PDF)

■ AUTHOR INFORMATION

Corresponding Authors

Tim Melin – Department of Chemistry, Ångström Laboratory, Uppsala University, SE-751 21 Uppsala, Sweden; orcid.org/0000-0001-6691-6706; Email: tim.melin@kemi.uu.se

Erik J. Berg – Department of Chemistry, Ångström Laboratory, Uppsala University, SE-751 21 Uppsala, Sweden; orcid.org/0000-0001-5653-0383; Email: erik.berg@kemi.uu.se

Author

Robin Lundström – Department of Chemistry, Ångström Laboratory, Uppsala University, SE-751 21 Uppsala, Sweden; orcid.org/0000-0001-9070-9264

Complete contact information is available at: <https://pubs.acs.org/doi/10.1021/acs.jpcllett.4c00328>

Notes

The authors declare no competing financial interest.

■ ACKNOWLEDGMENTS

The authors acknowledge Knut and Alice Wallenberg (KAW) Foundation (Grant 2017.0204) and Swedish Research Council (2016–04069) for financial support. StandUp for Energy is acknowledged for base funding.

■ REFERENCES

- (1) Xu, K. Electrolytes and Interphases in Li-Ion Batteries and Beyond. *Chem. Rev.* **2014**, *114*, 11503–11618.
- (2) Pieczonka, N. P. W.; Yang, L.; Balogh, M. P.; Powell, B. R.; Chemelewski, K.; Manthiram, A.; Krachkovskiy, S. A.; Goward, G. R.; Liu, M.; Kim, J. H. Impact of Lithium Bis(Oxalate)Borate Electrolyte Additive on the Performance of High-Voltage Spinel/Graphite Li-Ion Batteries. *J. Phys. Chem. C* **2013**, *117*, 22603–22612.
- (3) Li, J.; Yang, J.; Ji, Z.; Su, M.; Li, H.; Wu, Y.; Su, X.; Zhang, Z. Prospective Application, Mechanism, and Deficiency of Lithium Bis(Oxalate)Borate as the Electrolyte Additive for Lithium-Batteries. *Adv. Energy Mater.* **2023**, *13*, 2301422.
- (4) Lischka, U.; Wietelmann, U.; Wegner, M. German Patent DE 19829030 C1, 1999
- (5) Xu, K.; Zhang, S.; Poese, B. A.; Jow, T. R. Lithium Bis(Oxalato)Borate Stabilizes Graphite Anode in Propylene Carbonate. *Electrochem. Solid-State Lett.* **2002**, *5*, A259–A262.
- (6) Xu, K.; Zhang, S.; Jow, T. R.; Xu, W.; Angell, C. A. LiBOB as Salt for Lithium-Ion Batteries. A Possible Solution for High Temperature Operation. *Electrochem. Solid-State Lett.* **2002**, *5*, A26–A29.
- (7) Xu, K.; Lee, U.; Zhang, S.; Wood, M.; Jow, T. R. Chemical Analysis of Graphite/Electrolyte Interface Formed in LiBOB-Based Electrolytes. *Electrochem. Solid-State Lett.* **2003**, *6*, A144–A148.
- (8) Xu, K.; Zhang, S.; Jow, T. R. Formation of the Graphite/Electrolyte Interface by Lithium Bis(Oxalato)Borate. *Electrochem. Solid-State Lett.* **2003**, *6*, A117–A120.
- (9) Zhuang, G. V.; Xu, K.; Jow, T. R.; Ross, P. N. Study of SEI Layer Formed on Graphite Anodes in PC/LiBOB Electrolyte Using IR Spectroscopy. *Electrochem. Solid-State Lett.* **2004**, *7*, A224–A227.
- (10) Xu, K.; Lee, U.; Zhang, S.; Jow, T. R. Graphite/Electrolyte Interface Formed in LiBOB-Based Electrolytes: II. Potential Dependence of Surface Chemistry on Graphitic Anodes. *J. Electrochem. Soc.* **2004**, *151*, A2106–A2112.
- (11) Xu, K.; Zhang, S.; Jow, T. R. LiBOB as Additive in LiPF₆-Based Lithium Ion Electrolytes. *Electrochem. Solid-State Lett.* **2005**, *8*, A365–A368.
- (12) Larush-Asraf, L.; Biton, M.; Teller, H.; Zinigrad, E.; Aurbach, D. On the Electrochemical and Thermal Behavior of Lithium Bis(Oxalato)Borate (LiBOB) Solutions. *J. Power Sources* **2007**, *174*, 400–407.
- (13) Nie, M.; Lucht, B. L. Role of Lithium Salt on Solid Electrolyte Interface (SEI) Formation and Structure in Lithium Ion Batteries. *J. Electrochem. Soc.* **2014**, *161*, A1001–A1006.
- (14) Huang, S.; Wang, S.; Hu, G.; Cheong, L. Z.; Shen, C. Modulation of Solid Electrolyte Interphase of Lithium-Ion Batteries by LiDFOB and LiBOB Electrolyte Additives. *Appl. Surf. Sci.* **2018**, *441*, 265–271.

(15) Yang, L.; Furczon, M. M.; Xiao, A.; Lucht, B. L.; Zhang, Z.; Abraham, D. P. Effect of Impurities and Moisture on Lithium Bisoxalato-borate (LiBOB) Electrolyte Performance in Lithium-Ion Cells. *J. Power Sources* **2010**, *195*, 1698–1705.

(16) Xu, K.; Zhang, S. S.; Lee, U.; Allen, J. L.; Jow, T. R. LiBOB: Is It an Alternative Salt for Lithium Ion Chemistry? *J. Power Sources* **2005**, *146*, 79–85.

(17) Xu, K.; Lee, U.; Zhang, S.; Allen, J. L.; Jow, T. R. Graphite/Electrolyte Interface Formed in LiBOB-Based Electrolytes I. Differentiating the Roles of EC and LiBOB in SEI Formation. *Electrochem. Solid-State Lett.* **2004**, *7*, A273–A277.

(18) Choi, N. S.; Yew, K. H.; Kim, H.; Kim, S. S.; Choi, W. U. Surface Layer Formed on Silicon Thin-Film Electrode in Lithium Bis(Oxalato) Borate-Based Electrolyte. *J. Power Sources* **2007**, *172*, 404–409.

(19) Holomb, R.; Xu, W.; Markusson, H.; Johansson, P.; Jacobsson, P. Vibrational Spectroscopy and Ab Initio Studies of Lithium Bis(Oxalato)Borate (LiBOB) in Different Solvents. *J. Phys. Chem. A* **2006**, *110*, 11467–11472.

(20) Schwenke, K. U.; Solchenbach, S.; Demeaux, J.; Lucht, B. L.; Gasteiger, H. A. The Impact of CO₂ Evolved from VC and FEC during Formation of Graphite Anodes in Lithium-Ion Batteries. *J. Electrochem. Soc.* **2019**, *166*, A2035–A2047.